

1 **“Genome-wide population diversity in *Hymenoscyphus fraxineus* points to an eastern**  
2 **Russian origin of European Ash dieback”**

3

4 Jørn Henrik Sønstebo<sup>1†</sup>, Adam Vivian-Smith<sup>1</sup>, Kalev Adamson<sup>2</sup>, Rein Drenkhan<sup>2</sup>, Halvor  
5 Solheim<sup>1</sup> and Ari M. Hietala<sup>1</sup>

6 <sup>1</sup>Norwegian Institute of Bioeconomy Research, Pb 115, NO-1431 Ås, Norway

7 <sup>2</sup>Institute of Forestry and Rural Engineering (IFRE), Estonian University of Life Sciences,  
8 Tartu, Estonia

9 <sup>†</sup>Author for correspondence

10

11 **Abstract**

12 European forests are experiencing extensive invasion from the Ash pathogen *Hymenoscyphus*  
13 *fraxineus*, an ecological niche competitor to the non-pathogenic native congener *H. albidus*.  
14 We report the genome-wide diversity and population structure in Asia (native) and Europe  
15 (the introduced range). We show *H. fraxineus* underwent a dramatic bottleneck upon  
16 introduction to Europe around 30-40 generations ago, leaving a genomic signature,  
17 characterized by long segments of fixation, interspersed with “diversity islands” that are  
18 identical throughout Europe. This means no effective secondary contact with other  
19 populations has occurred. Genome-wide variation is consistently high within sampled  
20 locations in Japan and the Russian Far East, and lack of differentiation amongst Russian  
21 locations suggests extensive gene flow, similar to Europe. A local ancestry analysis supports  
22 Russia as a more likely source population than Japan. Negligible latency, rapid host-range  
23 expansion and viability of small founding populations specify strong biosecurity forewarnings  
24 against new introductions from outside Europe.

25

26 **Keywords:** population genomics, Helotiales, invasion, fungal evolutionary genomics,  
27 adaptive divergence

28

## 29 **Introduction**

30 Establishment likelihood and impact of an invasive species can be often associated by the  
31 ecological similarity of species assemblages at different locations (Paini et al. 2016), the  
32 presence of specific ecological drivers (Dawson et al. 2017), the number of introductions and  
33 the viability of small populations (Blackburn et al. 2011, Fauvergue et al. 2012).

34 Understanding evolutionary processes associated with biological invasions such as loss of  
35 genetic variation due to reduction in population size at the founder event and change in  
36 selection pressure in the new environment is challenging (Zhan et al. 2012), but necessary to  
37 comprehend the historical process and future trajectory of the invasion. Population genomic  
38 analyses use genome scale sequence data to enable the study of these evolutionary processes  
39 (Grunwald et al. 2016). Comparing the genome wide genetic structure and diversity between  
40 native and introduced populations enables detailed studies of the genetic and evolutionary  
41 aspects of the invasion. Principal questions to address are the number of introduction events,  
42 the mode of establishment, the initial effective population size, the effects of the founder  
43 event on the genetic structure and diversity, and the differences in adaptive potential between  
44 the native and the introduced populations.

45 Dieback of European Ash (*Fraxinus excelsior* L.) is one of the most important fungal  
46 diseases on trees in Europe as it threatens a keystone tree species and associated forest  
47 biodiversity. The causative ascomycete *H. fraxineus* appears to have been introduced to  
48 Europe from Asia, where similar parallel species assemblages exist. In Asia *H. fraxineus* is  
49 reported as extensive leaf colonizer and notably a weak pathogen of *Fraxinus mandshurica*  
50 and *F. rhynchophylla* (Zhao et al. 2013, Zheng and Zhuang 2014, Drenkhan et al. 2017). In  
51 contrast to its role as a leaf colonizer and weak pathogen on Asian ash species, *H. fraxineus* is  
52 able to grow into shoots and branches of European ash and eventually kill the tree. Young  
53 trees die within a few years of infection while older trees often become chronically infected  
54 (Kowalski and Holdenrieder 2009, Skovsgaard et al. 2010). European Ash has also been  
55 historically associated with a non-pathogenic endophyte *H. albidus* (Baral and Bemann  
56 2014, Baral et al. 2014), a species experiencing invasion-induced range contraction through  
57 direct niche competition (McKinney et al. 2012).

58 The *H. fraxineus* invasion relies on a high sexual ascospore production (Cross et al.  
59 2017), consistent with propagule pressure theory (Lockwood et al. 2005). The life cycle can  
60 be completed annually via the formation of apothecia on leaf petioles and rachis debris left on  
61 the forest floor (Kowalski and Holdenrieder 2009, Timmermann et al. 2011). Synchronous  
62 ascospore discharge (Hietala et al. 2013) appears to coordinate host challenge and facilitate

63 long distance dispersal, as proposed for other ascomycetes (Roper et al. 2010). While *H.*  
64 *fraxineus* is an outcrossing fungus with equal representation of the two mating types in  
65 Europe (Gross et al. 2012), it additionally produces asexual spores (Kowalski and  
66 Bartnik, 2010; Fones et al. 2016), but as no clonal populations occur these have been  
67 proposed to function primarily as spermatia (Gross et al. 2012). Gene introgression from  
68 native species may facilitate adaptation of invasive plant pathogens (Gonthier and Garbelotto  
69 2011), yet the population structures and relationships between *H. fraxineus* and the native  
70 competitor *H. albidus* have not been characterized at genome-wide scales.

71 Ash dieback symptoms were first recorded in Poland in the early 1990s (Przybył  
72 2002), and the first European record of *H. fraxineus* is from Estonia from 1997 (Drenkhan et  
73 al. 2016). Since 2001, extensive spread has been observed throughout Europe and into  
74 Scandinavia (McKinney et al. 2014). The disease front advanced in 1992-2008 from eastern  
75 Poland to Switzerland with an annual dispersal rate of 75 km per year (Gross et al. 2014).  
76 Genetic diversity and population structure studies have provided some broad indications about  
77 the spread of *H. fraxineus* in Europe (Rytönen et al. 2011, Bengtsson et al. 2012, Gross et al.  
78 2012, Kraj et al. 2012, Gross et al. 2014, Burokiene et al. 2015). Schoebel et al. (2017) also  
79 recently characterized the mitovirus population associated with *H. fraxineus* in Europe,  
80 showing the presence of two ancestral types, perhaps indicative of two founding parents.  
81 Together these prior studies provide a narrative that for a lack of population structure and low  
82 European allelic richness: as compared to Japanese populations on *F. mandshurica*, the  
83 European population was established by two individual strains in eastern Europe (Gross et al.  
84 2014), although few informative microsatellite loci have been studied.

85 Here we report, alongside McMullan et al. (submitted), who sequenced and assembled  
86 the *H. fraxineus* genome, the genome-wide diversity of multiple *H. fraxineus* populations in  
87 Europe, with reference sampling locations in Far Eastern Russia and Japan (Figure 1A,B),  
88 using densely spaced single nucleotide polymorphisms (SNPs). We support the conclusion of  
89 McMullan et al. (submitted) that only two haploid *H. fraxineus* individuals founded the  
90 European population, and show that this led to a genome-wide reduction in genetic diversity  
91 compared to the native populations. We show that the bottleneck experienced in the European  
92 population drastically reduced genetic diversity and caused fixation of large swathes of the  
93 genome, which are detected in all European samples. Importantly we use this data, along with  
94 the allelic richness and genetic differentiation in the Russian Far East and Japanese  
95 populations, to provide information about the potential for local adaptation, and estimate the

96 time since the introduction to Europe, and conclude, through a local ancestry analysis, that the  
97 Russian Far East is a likely source for the invasive population.

98

## 99 **Material and methods**

### 100 *Hymenoscyphus fraxineus* samples

101 Samples of *Hymenoscyphus fraxineus* were collected from Estonia (33 individuals), Norway  
102 (90) and the Russian Far East (51). Additional samples were obtained from Japan (5) and  
103 from other locations in Europe (14), including the holotype strain of *H. fraxineus* (see  
104 Supplementary Table 1). We analysed in total 193 *H. fraxineus* individuals. Estonia and  
105 Norway were specifically chosen as representative locations because of distinct disease  
106 histories. The first European record of *H. fraxineus* is from 1997 from Estonia (Drenkhan et  
107 al. 2016). In Norway, Ash dieback was first documented in southeastern parts of the country  
108 in 2008, after which the disease spread along the west coast at an annual rate of 51 km  
109 (Solheim and Hietala (2017); Figure 1A).

110 Sampling in Norway and Estonia was performed over several years, with Norway  
111 from 2008 to 2014 covering the disease fronts along the southern and western coasts  
112 (Supplementary Table1). Estonian sampling was conducted from 2010 to 2014, while the  
113 samples from the Russian Far East were collected in 2014 in three locations (Figure 1,  
114 Supplementary Table 1). The majority of Norwegian samples represent haploid monokaryotic  
115 isolates, with some obtained as a single spore cultures (SSC) from ascocarps, and some as a  
116 single hyphal isolates from mycelial *in vitro* cultures derived from necrotic shoot lesions  
117 (Supplementary Table 1). All Estonian and Russian samples were ascocarps, meaning they are  
118 heterokaryotic and contain the parental strains and sexual progeny. In addition to the *H.*  
119 *fraxineus* samples we also included five *H. albidus* isolates from Norway and Switzerland  
120 (Supplementary Table 1).

121

### 122 *ddRAD* analysis

123 DNA samples from all Estonian and the Russian Far East ascocarps were extracted using the  
124 E.Z.N.A Fungal DNA Mini Kit (Omega Bio-Tek Inc., Norcross, GA, USA). Norwegian DNA  
125 samples were isolated using the Easy-DNA protocol No. 8 for Mouse Tails (Thermo Fisher  
126 Scientific). DNA quantity was assessed with the Nanodrop 2000 (Thermo Fisher Scientific),  
127 and/or the Qubit DNA Broad Range Sensitivity assay (Thermo Fisher Scientific). Of the five

128 Japanese isolates, DNAs from three Japanese isolates were directly amplified from mycelia  
129 using the Repli-G Single Cell kit using whole genome amplification (P/N 150343; Qiagen;  
130 Supplementary methods and Supplementary Table 1).

131 All samples were pretested by species-specific ITS PCR and Sanger sequencing using  
132 HFrax-F and HFrax-R primers as described previously (Drenkhan et al. 2016, Cross et al.  
133 2017). All the samples were positive and provided typical alignments to *H. fraxineus* except  
134 for two samples from Russia and one Estonian sample (IDs 4054; 4142 and 4137  
135 respectively), which were excluded later after ddRAD sequencing, since these samples were  
136 contaminants from unrelated species (Supplementary Table 1).

137 Each DNA sample consisted of a normalized input of 200 ng, which was prepared in  
138 30 µl of nuclease free water. A single digestion and ligation reaction comprised the DNA with  
139 *PstI*-HF and *MspI* (New England Biolabs; R3140L and R0106L respectively) and the ddRAD  
140 ligation adapters compatible to the restriction sites together with 20 units of each restriction  
141 enzyme, 100 units of T4 DNA ligase and 1 µl of 10 mM ATP, in a total volume of 40 µl.  
142 Reactions were pooled and purified in the subsequent steps with 1.1x volumes of AmpureXP  
143 (Beckman Coulter, Inc.). Samples with compatible barcodes were size fractionated together to  
144 183 to 383 bp with the Pippin Prep and a 2% agarose gel cassette (2010CDS) using marker B  
145 (Sage Science, Beverly, MA, USA). Size selected libraries were further purified with  
146 AmpureXP and then amplified in a total volume of 260 µl with Platinum PCR Super Mix  
147 High Fidelity polymerase (Thermo Fisher), 10 µl each of the P and A1 primer (20 µM) as  
148 described in Ion Xpress library amplification (Thermo Fisher Scientific; Vivian-Smith and  
149 Sønstebo, 2017). Libraries were qualified and quantified using a Bioanalyzer 2100 High  
150 Sensitivity DNA chip (Agilent) before appropriately diluting the sample and populating Ion  
151 Sphere Particles (ISPs) with template. Emulsion PCR and enrichment of ISPs were either  
152 performed using the Ion One Touch 2 system using OT2 reagents (Thermo Fisher Scientific  
153 Publication Part Number MAN0007221 Rev. 2.0), or the Ion Chef using IC 200 reagents  
154 (MAN0007661 Rev. A.0). Sequencing was performed on an Ion torrent PGM sequencer using  
155 316 chips and monitored with FastQC (Leggett et al. 2013).

156  
157 *Bioinformatics*

158 The ddRAD sequences were de-multiplexed using Torrent Server software suite 4.6. The  
159 sequences from the individual samples were then quality trimmed in CLC Genomic  
160 Workbench 8 ([www.qiagenbioinformatics.com](http://www.qiagenbioinformatics.com)). Sequences passing this filter were mapped to

161 the reference genome KW1 *Hfv2* (Saunders et al. 2014, McMullan et al. submitted), using  
162 Novoalign (Novocraft Technologies, Selangor, Malaysia).

163 Multi-sample variant calling was performed with FREEBAYES (Garrison and Marth  
164 2012), with --min-alternate-count 4 --min-alternate-fraction 0.2. Given the generally higher  
165 rate of errors in indels compared to SNPs in Ion Torrent data, we filtered out all the indels and  
166 kept only the SNPs in the further analyses. This was done using VCFILTER in VCFLIB  
167 (<https://github.com/vcflib/vcflib>), where also only variants with a QUAL score above 30 were  
168 retained. SNPs present in less than 20% of the individuals were removed as well as SNPs with  
169 a minor allele frequency (MAF) of less than 1%. The MAF was set low since many of the loci  
170 that are monomorphic in Europe show variation in the Asian population. Increasing the limit  
171 of the MAF to 0.05 led to many of the Asian specific alleles being lost. Filtering of SNPs was  
172 performed in VCFTOOLS (Danecek et al. 2011). The SplitsTree (Huson and Bryant 2006)  
173 and the STRUCTURE v2.3.4 (Pritchard et al. 2000, Falush et al. 2003) analysis (see below)  
174 was performed on a thinned data set, at one marker per contig, using the thinning procedure in  
175 VCFTOOLS.

176

### 177 *Population genomic analysis*

178 McMullan et al. (submitted) detected a highly reduced genetic diversity in European *H.*  
179 *fraxineus* throughout the genome compared with the Japanese population, suggesting that the  
180 European population was founded by a few individuals. In order to confirm this, we  
181 calculated the nucleotide diversity in the R-package PopGenome (Pfeifer et al. 2014) for each  
182 population, except Japan, for which too few isolates were available. The calculations were  
183 done in windows of seven SNPs with a step of five SNPs. The pattern of nucleotide diversity  
184 was also assessed with the calculation of nucleotide divergence  $\pi$  in VCFTOOLS (Danecek et  
185 al. 2011). Here,  $\pi$  was calculated over sliding windows of 20 kb with 5 kb steps. We  
186 combined all samples from Europe to contain the overall diversity in Europe and compared  
187 that with all Russian samples.

188 Tajima's D was used to detect departures from the standard neutral model and  
189 calculated using VCFTOOLS (Danecek et al. 2011).

190 To further assess signature of selection, we used the Bayesian likelihood method  
191 implemented via reversible jump Markov Chain Monte Carlo in BayeScan (Foll and Gaggiotti  
192 2008). In short, BayeScan estimates the probability that a locus is under selection by  
193 calculating a Bayes factor, which is simply the ratio of the posterior probabilities of two  
194 models (selection/neutral) in the given data. Bayes factors above 100 ( $\log_{10} > 2$ ) correspond

195 to posterior probabilities between 0.99 and 1. BayeScan has been shown to detect most loci  
196 under strong selection, with low probability of detecting false positive (Narum and Hess  
197 2011). The BayeScan analysis was performed separately in Europe and Asia. In Europe we  
198 divided the Norwegian population into an Eastern (early introduction) and a Western (later  
199 introduction) population and used these along with the Estonian population to detect selection  
200 (the groups are described in Supplementary Table 1). In Asia we used the three sampling  
201 locations as populations and used these to infer loci under selection.

202 The relationship among samples of *H. fraxineus* and *H. albidus* were investigated with  
203 principle component analyses (PCA) in the R package SNPRelate (Zheng et al. 2012), using  
204 only loci with a level of linkage disequilibrium  $r$  smaller than 0.2. We also performed a  
205 phylogenetic network analysis using the Neighbor-Net algorithm in SplitsTree 4.0 (Huson and  
206 Bryant 2006). Concatenated SNPs were extracted from the VCF file using PGDSpider  
207 (Lischer and Excoffier 2012). SplitsTree was performed using uncorrected P distances and the  
208 heterozygous sites were treated as average between the two alternative states. In both the PCA  
209 and SplitsTree analysis we included *H. albidus* as an outgroup, but also to examine signs of  
210 hybridization between the two species. The genetic differentiation between the two species  
211 and among sampling locations within *H. fraxineus* was also investigated with sliding window  
212  $F_{ST}$  analyses along the genome (100kb windows, 50kb steps) using VCFTOOLS.

213 The genetic structure of *H. fraxineus* was assessed using STRUCTURE v2.3.4  
214 (Pritchard et al. 2000, Falush et al. 2003). In STRUCTURE, individuals are placed into K  
215 clusters that are in H-W and linkage equilibrium, and have distinctive allele frequencies  
216 without imposing *a priori* population information. K was chosen in advance, but was varied  
217 between 1 and 6. For each K value the analysis was iterated 20 times using an initial burn-in  
218 of 50 000 cycles, and then another additional 50 000 cycles. Individuals may have  
219 membership in several clusters (indicating admixture) with the membership coefficient  
220 summing to 1. STRUCTURE output,  $\Pr(X|K)$ , can be used as an indication of the most likely  
221 number of genetic groups and the level of admixture between groups. However, as indicated  
222 in the STRUCTURE documentation and according to Evanno et al. (2005),  $\Pr(X|K)$  plateaus  
223 or slightly increases after the best K is reached. Thus, following Evanno et al. (2005), deltaK  
224 was calculated and used to evaluate the most probable genetic structure. Delta K was  
225 calculated using STRUCTURE HARVESTER (Earl and vonHoldt 2012) and runs with  
226 identical K were combined with CLUMPP (Jakobsson and Rosenberg 2007). Finally  
227 PCAdmix was used to infer local ancestry (Brisbin et al. 2012). This approach relied on  
228 phased haplotypes derived from both reference panels and the admixed individuals. We used

229 Beagle 4.0 (Browning and Browning 2007) to phase the data from ascocarps, without  
230 imputation. This was done individually for each population. The local ancestry was inferred  
231 with PCAdmix using windows of 10 SNPs. For each window, the distribution of individual  
232 scores within a population is modeled by fitting a multivariate normal distribution. These  
233 distributions are then used to compute the likelihood of each score belonging to either Japan  
234 or Russia. Local ancestry assignments were determined using a 0.9 posterior probability  
235 threshold for each window. Samples having probability of belonging to a reference of  $< 0.9$   
236 were recorded as missing ancestry.

237

## 238 **Results**

239 ddRAD sequencing provided an almost uniform coverage across the *H. fraxineus* genome  
240 (Supplementary Figure 1), and an average of 0.86% total of the genome was consistently  
241 resequenced at each ddRAD loci for each sample. Small tracts of the genome that represented  
242 specific sequence compositions that did not cut with *PstI* and *MspI* were under-sampled, the  
243 largest being around 250 kbp (Supplementary Figure 1; scaffold 13). The amounts of reads  
244 that mapped to the genome also varied between samples (Supplementary Figure 2), but in  
245 general, 90% of the reads in each of the European and Japanese mycelial cultures mapped to  
246 the Hfv2 genome (McMullan et al., submitted). Lower levels of the *H. fraxineus* ascocarp  
247 reads mapped and we observed a larger variation in the percentage of mapped reads per  
248 individual. For the *H. albidus* cultures around 75% of the reads mapped to the *Hfv2* reference  
249 genome (Supplementary Figure 2). BLAST searches from the unmapped reads from the  
250 ascocarps detected contaminants such as *Pseudomonas aeruginosa*. The variant calling with  
251 FREEBAYES detected in total 71335 variable sites of which 49019 were SNPs. After  
252 removing SNPs with a maximum amount of missing data of 0.2 (44564 left) and a minimum  
253 allele frequency  $< 0.01$ , 15181 SNPs were left for further analyses.

254

## 255 ***H. fraxineus* and *H. albidus* are well separated species**

256 Principle component analysis separated *H. fraxineus* and *H. albidus* along the first  
257 eigenvector, which held 7.25 percent of the variance (Figure 1C). The clear separation  
258 between *H. fraxineus* and *H. albidus* was also evident in the SplitsTree analyses where all the  
259 *H. fraxineus* individuals were separated from *H. albidus* with a single long branch containing  
260 both the Swiss and Norwegian isolates (Supplementary Figure 3). Similarly the  $F_{ST}$  analysis  
261 showed a high differentiation between European or Asian *H. fraxineus* and *H. albidus*: mean



262 pairwise  $F_{ST}$  for *H. albidus* and European or Asian *H. fraxineus* were 0.767 (sd 0.208) and  
263 0.420 (sd 0.243), respectively. This pattern was consistent across all scaffolds (Supplementary  
264 Figure 4) suggesting that introgression between the two species has not taken place or the  
265 level is too low to be detected by these analyses. However, European *H. albidus* is  
266 additionally differentiated from *H. fraxineus* based on a preliminary genomic resequencing  
267 analysis and mapping of *H. albidus* sequencing reads to *Hfv2* scaffolds (Vivian-Smith, pers.  
268 comm.). Comparisons of the total GC content and a K-mer analysis, show consistent  
269 differences between the two species (Supplementary Figure 5). Therefore, the population  
270 structure analyses, together with preliminary genomic data, unambiguously resolves *H.*  
271 *albidus* into a separate species.

### 272 **Population structure analyses show clear division of native and introduced *H. fraxineus*** 273 **populations, with a variable level of structuring between two biogeographic regions**

274 The genome-wide PCA divided the Asian and the European samples of *H. fraxineus* into two  
275 clearly separated groups along the first eigenvector, while the second eigenvector mainly  
276 showed variation in the Asian individuals (Figure 1D). In comparison, the single-scaffold  
277 PCA also separated the European and the Asian samples along the first axis for all scaffolds  
278 (Supplementary Figure 6), but their differentiation was much weaker than in the genome-wide  
279 PCA (Figure 1D). The clear distinction between the Asian and the European populations was  
280 also found in the neighbor-network SplitsTree analysis, where the Asian and European groups  
281 connected with a few long parallel branches (Figure 1E). Strains from Japan were embedded  
282 in the Russian group, but had longer branches than the samples from Russia, which may be  
283 due to origin at widely different locations in Japan. In the European group, all isolates were  
284 largely connected at one node potentially representing a single common ancestor at the  
285 foundation of the European population, a finding which is reinforced when the Neighbor-Net  
286 split decomposition analysis is performed with only the European isolates (Supplementary  
287 Figure 7). STRUCTURE analysis with  $K = 2$  also realized that two genetic groups were  
288 almost exclusively divided between Asia and Europe (not shown).

289 Separation between Japanese and Russian populations was detected in the PCA  
290 analysis when STRUCTURE was performed on only the Asian samples (Figure 2). With  $K=2$   
291 the Asian samples divided into a Japanese and a Russian group with very little admixture.  
292 With  $K=3$  a third group was observed that had a slightly variable frequency across the three  
293 Russian survey locations. Within Europe, STRUCTURE detected two groups that were not  
294 related to geography or the time since local introduction. These groups are suspected to

295 represent the two historical parental haplotypes that founded the European population, with  
296 each group displaying the residual allele frequency of the two original parental haplotypes.

297

### 298 **European populations show a fixation signature across the majority of scaffolds.**

299 The magnitude of the genome-wide reduction in nucleotide diversity varied considerably  
300 amongst scaffolds, but an identical pattern was discovered throughout all three European  
301 populations (Figure 3). In contrast, populations from Russia had a high genome-wide  
302 nucleotide diversity (Figure 3). We considered that the regions of low nucleotide diversity  
303 were the tracts of the genome where fixation event(s) had occurred and termed the regions  
304 with higher nucleotide “diversity islands”. Several scaffolds appeared to have entirely  
305 preserved their former diversity and escaped fixation (scaffolds 13 and 15; Figure 3). Other  
306 scaffolds have almost been exclusively fixed (scaffolds 14, 16 and 20). Similar pattern was  
307 observed in the  $\pi$  calculated in windows of 20 kb (Supplementary Figure 8). However, we did  
308 observe several small diversity islands within these chromatids. These were either  
309 representative of a close and coincident double recombinant event, or a set of sequential inter-  
310 generational recombinant events that then led to fixation on either side of the diversity island.  
311 The proportion of smaller diversity islands throughout the genome (Figure 3), along with the  
312 near complete fixation of entire chromatids, further denote that the fixation event occurred in  
313 a succinct and sequential manner after immigration. Importantly, this occurred prior to the  
314 European *H. fraxineus* isolate becoming numerically superior and spreading throughout the  
315 whole European region, thus leaving a fixation signature homogenous to the whole of Europe.

316 The pattern of segmentation for the fixed tracts and diversity islands, which is  
317 expected to be a signature of a bottleneck from the founding population, yields information on  
318 the establishment phase and breeding behavior. Therefore, each of the fixed segments, and  
319 diversity islands was assessed for the length of that tract and their occurrence frequencies at  
320 by calculation in R (Supplementary Methods). The average length of the fixed blocks was 68  
321 Kbp, with a maximum spanning length of 1.13 Mbp. Likewise, the average length of the  
322 polymorphic blocks was 54.6 Kbp, with a maximum spanning length of 245 Kbp  
323 (Supplementary Figure 9). It follows that the timing since the fixation event can be  
324 approximated based on the level of recombination and the subsequent fragmentation of the  
325 genome into non-variable segments (Stukenbrock et al. 2011, Stukenbrock et al. 2012), even  
326 though these segments will have aggregated to a certain extent. Estimates of recombination  
327 rates for ascomycetous fungi range from 46 cM/Mb in an ancestral type of *Zymoseptoria*  
328 (*Dothideomycetes*), to between 86 and 128 cM/Mb for *Botrytis cinerea* (*Helotiales*);

329 (Amselem et al. 2011, Van Kan et al. 2017)). Taking the mean 68 Kbp size of the non-  
330 variable segments of the European *H. fraxinus* as a chronicle of the historical recombination  
331 process since the fixation event, it can be postulated that if a recombination event occurred  
332 every 2.2 Mb per generation (Stukenbrock et al. 2012), then the time since fixation is 32  
333 generations/years. Taking the mean of 98.6 cM/Mb for *Botrytis cinerea* as a proxy leads to an  
334 estimate of around 14 years. Likewise, estimates from the variable segments provide estimates  
335 of 40.3 years, and 18.6 years given the recombination rates of 46cM/Mb and 98.6 cM/Mb as  
336 observed in *Zymoseptoria* sp. and *Botrytis cinerea* respectively. While this data does not  
337 identify the contribution of ancestral haplotypes to the non-variable segments, the data  
338 provided an opportunity to estimate the total proportion of the genome under fixation. This  
339 stands at 55.2%, and indicates some particular limitations on inter-generational breeding.  
340 Importantly, the parental strains appear to have been labile and characteristic of an annual life  
341 cycle, and the two founding individuals did not provide a continued contribution to the next  
342 generation, so a portion of their genetic contribution was lost through the fixation event.

343

#### 344 **European genetic diversity is bottlenecked but the potential exists for local adaptation**

345 McMullan et al (submitted) suggested, based on the diversity in effector genes that adaptive  
346 potential was still present in Europe. In order to compare the level of local adaptation in  
347 Europe and Asia we performed outlier analyses with BAYESCAN for the set of sampling  
348 sites in Europe (Estonia, eastern Norway and western Norway) and for the three Russian  
349 sampling sites. The populations in Europe and Russia had a similar genetic differentiation  
350 (Supplementary Figure 10), but the populations in Europe covered a larger biogeographical  
351 distance with different climatic zones. We detected 34 loci, dispersed across several scaffolds,  
352 with significant outlier behavior in Europe (corresponding to P value = 0.05). Of these 29 had  
353 P-values < 0.01, compared with only five in Russia, suggesting that local adaptation has  
354 already occurred since the introduction to Europe.

355 The average Tajima's D for each scaffold varied considerably in Europe, from -1.35  
356 within scaffold 14 to 0.91 in scaffold 15 (Figure 4). A positive Tajima's D in single genetic  
357 regions is evidence for heterozygous sites having a selective advantage, while negative values  
358 suggest directional selection for specific allele. If, however, the majority of the genome has  
359 either a negative or a positive Tajima's D value, the most probable explanation is that the  
360 population underwent a recent expansion or a bottleneck, respectively. In general, Tajima's D  
361 was negative for the scaffolds with low nucleotide variation and for the large blocks fixed for  
362 one allele, while it was positive for the polymorphic scaffolds (Figure 4). The positive

363 Tajima's  $D$  at the polymorphic loci probably reflects the founder event and the loss of rare  
364 alleles upon this event. The negative value in the monomorphic scaffolds may be a result of  
365 new mutations with low frequency, reflecting the recent increase in population size.

366

### 367 **European *H. fraxineus* comes from a locality near the Russian Far East**

368 The population structure detected in Europe may have been amplified by the strong genetic  
369 drift and extensive linkage disequilibrium experienced by the European population of *H.*  
370 *fraxineus* during and after the founder event as is evident from the genome wide loss in  
371 genetic diversity (Figure 3). Also, although the European group appeared highly diverged  
372 from the Asian populations in both the PCA, SplitsTree and the STRUCTURE analysis, only  
373 a total of 784 alleles were private to Europe, while 1178 were private to the five Japanese  
374 samples and 8244 alleles were private to Asia (Figure 5). In total 978 alleles were shared  
375 among Norwegian, Estonian and Russian samples, but absent in Japan, while 77 alleles were  
376 found in only Norway, Estonia and Japan. This suggests a closer relationship between Europe  
377 and Russia, than Europe and Japan.

378 In strong founder events, the low effective population size will affect the level of  
379 genetic drift and linkage disequilibrium resulting often in large changes in allele and  
380 haplotype frequencies. In order to infer the ancestry of the European samples we performed a  
381 local ancestry assignment using PCAdmix with Russia and Japan as ancestral groups. The  
382 local ancestry assignment was performed with PCAdmix in windows of ten SNPs along the  
383 genome for Norway and Estonia separately shows that a much closer Russian ancestry of the  
384 European samples is observed (for both Norwegian and Estonian), than towards the Japanese  
385 isolates (Figure 6). This corresponds well with the number of shared alleles found amongst  
386 these populations. Since the ancestral admixture assignment in PCAdmix examines the  
387 ancestry of small windows of SNPs it will be less affected by the changes in haplotype  
388 frequencies resulting from the genetic drift and linkage disequilibrium in the founding  
389 population. However, the results from the PCAdmix ancestry analysis were not homogenous  
390 throughout the genome. While the majority of windows had highest probability of a Russian  
391 origin, around 10% had Japan as the likely origin. These included portions of scaffolds 17, 9,  
392 8, 6, 4, 3 and 2. Since the number of individuals used in the analysis was much higher for  
393 Russia than Japan we performed an analysis with similar numbers of random Russian  
394 haplotypes as the Japanese (5). This increased the Japanese ancestry in the genome to around  
395 15%. Even though the fixed tracts of the European genome have not yet been assigned a  
396 parental haplotype group, smaller amounts of Japanese origin are likely explained by an

397 ancestral introgression event in the native population preceding the introduction to Europe, or  
398 alternatively that the European ancestral population is located slightly closer to Japan than  
399 those sites sampled in Russia.

400

## 401 **Discussion**

### 402 **Origin of European isolates of *H. fraxineus***

403 Genome-wide population diversity analysis using ddRAD allows increased sampling effort  
404 (increasing power), and provided important information on all stages of the invasion pathway  
405 including the introduction, the local establishment phase and the spread of *H. fraxineus*  
406 throughout Europe. The present study confirms the findings of McMullan et al., (submitted),  
407 that two parental individuals of *H. fraxineus* generated a self-sustaining population but in  
408 addition, the data presented here shows that these progenies then underwent a brief  
409 establishment phase and then swept throughout Europe in a short period of time. We suggest  
410 that *H. fraxineus* was introduced from the Russian Far East 14-32 years before the range  
411 expansion, which initiated probably around the time when the first symptoms occurred in the  
412 early 1990's (Przybył 2002). Our results establish that *H. fraxineus* has a low introduction  
413 effort but also that no other effective secondary contact occurred during the range expansion  
414 process.

415 The Russian Far East ancestry of the European *H. fraxineus* was much more likely than an  
416 ancestry directly from Japan. In addition to Japan and the Russian Far East, *H. fraxineus* has  
417 been found on both *Fraxinus mandshurica* and *F. rhynchophylla* in South Korea (Han et al.  
418 2014) and on *Fraxinus mandshurica* in China (Zheng and Zhuang 2014). Both the large  
419 number of fixed genomic regions, the lack of genetic structure and the presence of two  
420 haplotypes (McMullan et al (submitted)) show that *H. fraxineus* went through a severe genetic  
421 bottleneck upon introduction to Europe. Importantly we show that in the absence of secondary  
422 introductions since the founder event, 55% of the pathogen genome has become fixed and this  
423 signature is found throughout Europe. Effects of a founder event are such that alleles that are  
424 rare in the source population may be fixed upon introduction, through genetic drift. Such a  
425 scenario could explain the difference in the predominant ITS (internal transcribed spacer of  
426 rDNA) genotype between Europe and Asia (Drenkhan et al. 2017). Given the Japanese  
427 assignment of 10% - 15% of the European *H. fraxineus* genome, we cannot completely rule  
428 out that one isolate with a Japanese origin participated in the foundation of the European  
429 population. However, the fixed segments in the genome suggest that longer tracts with  
430 Japanese ancestry would probably be identified if this were the case. Thus it is much more

431 likely that an introgression of Japanese ancestry occurred in the native population before  
432 introduction into Europe. Broader sampling of the native range of *F. mandshurica* and *F.*  
433 *rhynchophylla* may lead to the identification of a closer Asian source to European population,  
434 although this may be complicated by the signal of high gene flow in eastern Asia. Similar  
435 genetic structure was detected with microsatellites in Japan (Gross et al. 2014). Drenkhan et  
436 al. (2014) found evidence for import of the Russian *Fraxinus mandshurica* from the Far East  
437 into Baltic countries during Soviet occupation, supporting this as a possible route of  
438 introduction. In particular, *Fraxinus mandshurica* seeds and plants were imported to Estonia  
439 from the 1960s to 1980s. *H. fraxineus* has been identified on seeds on both *F. excelsior* and *F.*  
440 *mandshurica* using species specific primers (Cleary et al. 2013, Drenkhan et al. 2017),  
441 suggesting seeds as a possible path of introduction. Although the pathogen DNA is present in  
442 the seeds it has proved difficult to isolate the fungus from this material (Drenkhan, pers  
443 communication). Even if *H. fraxineus* may have been spread by seeds, the highest risks, and  
444 most obvious route, would be through the movement of plant material such as seedlings and  
445 wood that support sexual or asexual proliferation of the fungus (Husson et al. 2012, Gross et  
446 al. 2014). Based on the length of the diversity islands (or fixed blocks), we estimated the  
447 introduction of *H. fraxineus* occurred 14-32 years before the range expansion in Europe  
448 started, which overlaps well with the period of importation for *F. mandshurica* (Drenkhan et  
449 al. 2014). While this estimate is reliant on recombination rate, we believe that the  
450 recombination rate from *Botrytis cinerea* is probably closer to the expected rate in *H.*  
451 *fraxineus*, since the species both belong to the fungal order Helotiales. This suggests a  
452 scenario where as few as two haplotypes of *H. fraxineus* arrived in Europe in the 1970's or the  
453 early 1980's, when the Baltic States were still a part of the Soviet Union and the population  
454 increased locally before expansion outside the area of introduction.

455         Although there has been a dramatic change in genetic diversity during the founder  
456 event a relatively large amount of variation has been retained within the diverse regions.  
457 McMullan et al (submitted) found that part of the diversity of effector genes was preserved in  
458 the European population due to the introduction of two divergent haplotypes. Similarly, we  
459 found relatively high numbers of loci were outlier loci that are potentially under selection in  
460 the different regions in Europe, suggesting that *H. fraxineus* has further potential for local  
461 adaptation. Further studies are needed to ascertain the function of the regions under selection.  
462 Local adaptation to differences in climate were detected in recent range expansions of  
463 *Cryphonectria parasitica* in France; isolates from northern France showed growth optima at

464 lower temperatures than those from southern France signifying that local adaptation evolved  
465 in a relatively short time (Robin et al. 2017).

466 The native European *Hymenoscyphus albidus*, which is a harmless leaf associate of  
467 European Ash (Baral and Bemmann 2014) could serve as a source of new genetic variation if  
468 hybridization occurs. However, no hybridization occurred in inter-specific crosses and *H.*  
469 *albidus* appears to reproduce exclusively via haploid selfing (Wey et al. 2016). These results  
470 are congruent with our genome-wide analysis which shows no signs of sexually or  
471 parasexually mediated introgression from *H. albidus* into the *H. fraxineus* genome. Our  
472 preliminary data on the genetic diversity of *H. albidus* suggests that the predominant mode of  
473 reproduction is selfing since very little variation was observed in the examined isolates from  
474 both Norway and Switzerland. More likely is that the niche-specialist *H. albidus* is just being  
475 solely outcompeted for the same sporulation niche and vastly overwhelmed by the mass of  
476 airborne *H. fraxineus* ascospores (Hietala et al. 2013).

477

#### 478 **Biosecurity of *H. fraxineus***

479 The European pathogen population is bottlenecked and so movement of the host within  
480 Europe is unlikely to impact the allele frequencies. A real concern is a novel immigration  
481 event; even the introduction of a single isolate from outside of the European area, from  
482 locations such as Japan and Far Eastern Russia, could dramatically alter the genetic diversity  
483 of the Ash pathogen. Predictive modelling and an assessment of the likelihood of arrival are  
484 required to understand the impact of this introgression into the European area. We would like  
485 to emphasize the role of sexual reproduction and gene flow as a mechanism to introduce  
486 immigrant variation into the European *H. fraxineus* population. Such a scenario might  
487 dramatically increase pathogen fitness and impose further selection pressure and a steeper  
488 decline on the European host.

489 Declining European Ash populations and further fragmentation of the natural ranges of Ash,  
490 as well as the presence of resistance in host range margins (Tollefsrud et al. 2016), may  
491 inhibit the establishment of new hybrid *H. fraxineus* types. Nonetheless, the European *H.*  
492 *fraxineus* invasive range is extensive, and expanding. Presently, bioclimatic niche models for  
493 invasive alien species are fundamental tools used for pest risk assessment (Guisan and  
494 Thuiller 2005, Kriticos et al. 2013). We believe that defining the genomic diversity of the  
495 invasive species in both the invaded and native ranges is similarly essential. The genetic  
496 diversity of this pathogen may already impact its ability to adapt to host selective pressures.

497 However, the pathogen's success in Europe, given the extreme nature of the primary founder  
498 event, reflects the fragility of Ash ecosystem. The present analysis was assisted by a fast  
499 sensitive surveillance and detection of genome-wide variation by scans gathered using  
500 ddRAD sequencing. This work, along with a refinement in the identification of the source  
501 population, will enable biosecurity managers to prioritize and make key decisions over  
502 resource management and assets, and to mitigate damage from Ash dieback, as well as for  
503 breeding an Ash recovery and future pest risk assessments.

504

#### 505 **Author contributions**

506 JHS, AVS, AH and HS designed the experiment. AH, HS, RD and KA collected the field  
507 material. AVS, JHS, AH, KA and RD performed DNA extractions and sequencing. JHS, AVS  
508 performed bioinformatic analysis. JHS, AVS and AH wrote the manuscript and with revisions  
509 from all authors.

#### 510 **Acknowledgments**

511 Financial contribution has been given by The Norwegian Genetic Resource Centre, The  
512 Research Council of Norway (grants 203822/E40 and 235947/E40), the Norwegian Financial  
513 Mechanism 2009–2014 under the project EMP162, the Institutional Research Funding IUT21-  
514 04, EMU project P170053MIMK, COST Action 1103 FRAXBACK and the Ministry of  
515 Agriculture and Food (131001).

516 We thank Dr Mark McMullan, Dr Matthew D. Clark, the NORNEX and OADB consortia for  
517 constructive comments and for sharing genomic data used in this study. We also thank Olaug  
518 Olsen and Gro Wollebæk (NIBIO), the laboratory of Prof Makoto Kakishima (Tsukuba,  
519 Japan), and the CBS-KNAW Fungal Biodiversity Centre (Utrecht, The Netherlands), for  
520 culturing and isolates, and Anne B. Nilsen and Jørn Petter Storholt (NIBIO) for GIS  
521 assistance.



## 522 **References**

- 523 Amselem, J., C. A. Cuomo, J. A. L. van Kan, et al. "Genomic Analysis of the Necrotrophic Fungal  
524 Pathogens *Sclerotinia sclerotiorum* and *Botrytis cinerea*." *PLOS Genetics* **7**: e1002230(2011).
- 525  
526 Baral, H.-O. & M. Bemann. "*Hymenoscyphus fraxineus* vs. *Hymenoscyphus albidus* – A comparative  
527 light microscopic study on the causal agent of European ash dieback and related foliicolous, stroma-  
528 forming species." *Mycology* **5**: 228-290(2014).
- 529  
530 Baral, H.-O., V. Queloz & T. Hosoya. "*Hymenoscyphus fraxineus*, the correct scientific name for the  
531 fungus causing ash dieback in Europe." *IMA Fungus* **5**: 79-80(2014).
- 532  
533 Bengtsson, S. B. K., R. Vasaitis, T. Kirisits, et al. "Population structure of *Hymenoscyphus*  
534 *pseudoalbidus* and its genetic relationship to *Hymenoscyphus albidus*." *Fungal Ecology* **5**: 147-  
535 153(2012).
- 536  
537 Blackburn, T. M., P. Pysek, S. Bacher, et al. "A proposed unified framework for biological invasions."  
538 *Trends in Ecology & Evolution* **26**: 333-339(2011).
- 539  
540 Brisbin, A., K. Bryc, J. Byrnes, et al. "PCAdmix: Principal Components-Based Assignment of Ancestry  
541 along Each Chromosome in Individuals with Admixed Ancestry from Two or More Populations."  
542 *Human biology* **84**: 343-364(2012).
- 543  
544 Browning, S. R. & B. L. Browning. "Rapid and accurate haplotype phasing and missing-data inference  
545 for whole-genome association studies by use of localized haplotype clustering." *American Journal of*  
546 *Human Genetics* **81**: 1084-1097(2007).
- 547  
548 Burokiene, D., S. Prospero, E. Jung, et al. "Genetic population structure of the invasive ash dieback  
549 pathogen *Hymenoscyphus fraxineus* in its expanding range." *Biological Invasions* **17**: 2743-  
550 2756(2015).
- 551  
552 Cleary, M. R., N. Arhipova, T. Gaitnieks, et al. "Natural infection of *Fraxinus excelsior* seeds by *Chalara*  
553 *fraxinea*." *Forest Pathology* **43**: 83-85(2013).
- 554  
555 Cross, H., J. H. Sønstebo, N. E. Nagy, et al. "Fungal diversity and seasonal succession in ash leaves  
556 infected by the invasive ascomycete *Hymenoscyphus fraxineus*." *New Phytologist* **213**: 1405-  
557 1417(2017).
- 558  
559 Danecek, P., A. Auton, G. Abecasis, et al. "The variant call format and VCFtools." *Bioinformatics* **27**:  
560 2156-2158(2011).
- 561  
562 Dawson, W., D. Moser, M. van Kleunen, et al. "Global hotspots and correlates of alien species  
563 richness across taxonomic groups." *Nature Ecology and Evolution* **1**: 0186(2017).

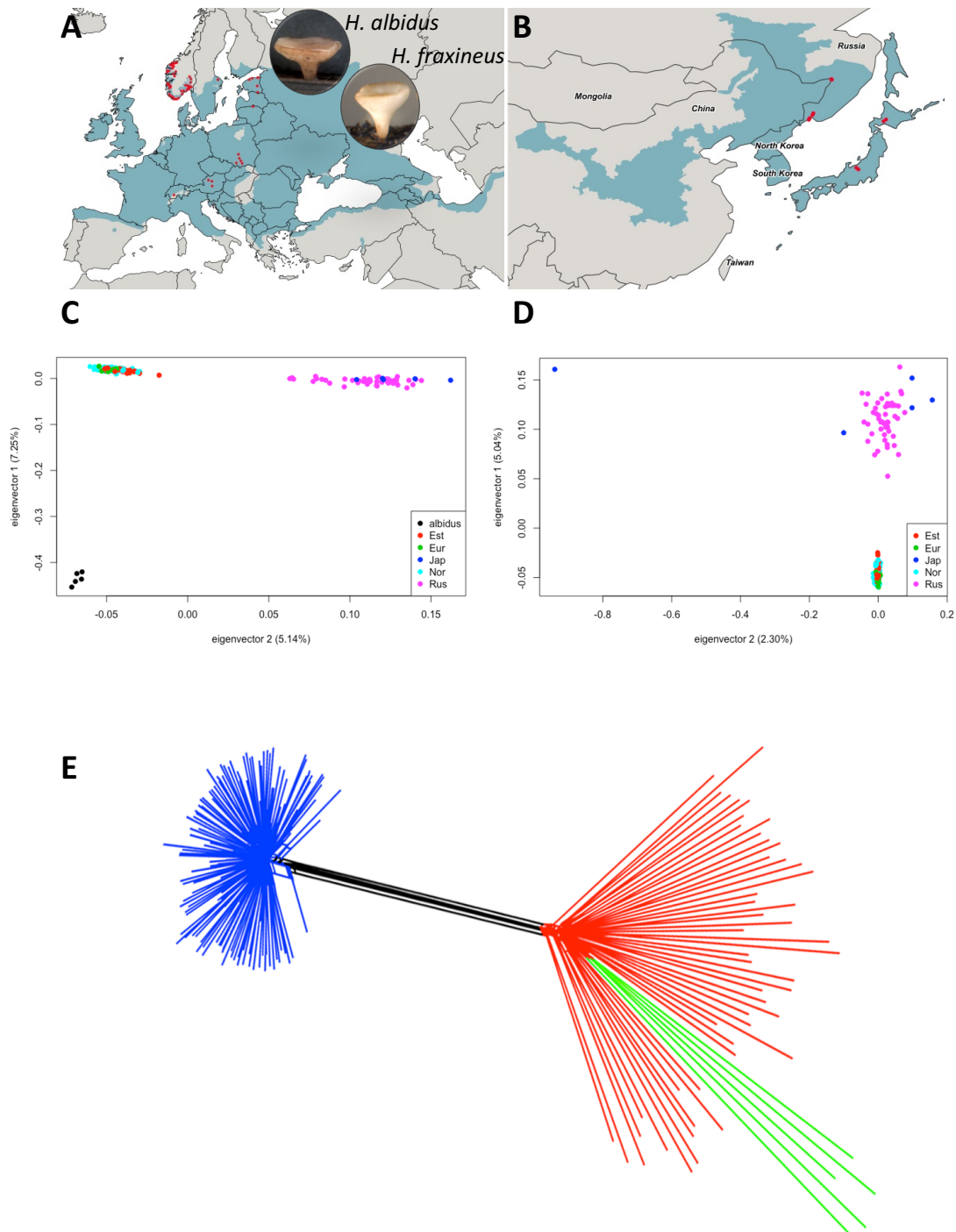
- 564  
565 Drenkhan, R., T. Riit, K. Adamson, et al. "The earliest samples of *Hymenoscyphus albidus* vs. *H.*  
566 *fraxineus* in Estonian mycological herbaria." *Mycological Progress* **15**: 835-844(2016).
- 567  
568 Drenkhan, R., H. Sander & M. Hanso. "Introduction of Mandshurian ash (*Fraxinus mandshurica* Rupr.)  
569 to Estonia: Is it related to the current epidemic on European ash (*F. excelsior* L.)?" *European Journal*  
570 *of Forest Research* **133**: 769-781(2014).
- 571  
572 Drenkhan, R., H. Solheim, A. Bogacheva, et al. "*Hymenoscyphus fraxineus* is a leaf pathogen of local  
573 *Fraxinus* species in the Russian Far East." *Plant Pathology* **66**: 490-500(2017).
- 574  
575 Earl, D. A. & B. M. vonHoldt. "STRUCTURE HARVESTER: a website and program for visualizing  
576 STRUCTURE output and implementing the Evanno method." *Conservation Genetics Resources* **4**: 359-  
577 361(2012).
- 578  
579 Evanno, G., S. Regnaut & J. Goudet. "Detecting the number of clusters of individuals using the  
580 software STRUCTURE: a simulation study." *Molecular Ecology* **14**: 2611-2620(2005).
- 581  
582 Falush, D., M. Stephens & J. K. Pritchard. "Inference of population structure using multilocus  
583 genotype data: Linked loci and correlated allele frequencies." *Genetics* **164**: 1567-1587(2003).
- 584  
585 Fauvergue, X., E. Vercken, T. Malausa, et al. "The biology of small, introduced populations, with  
586 special reference to biological control." *Evolutionary Applications* **5**: 424-443(2012).
- 587  
588 Foll, M. & O. Gaggiotti. "A Genome-Scan Method to Identify Selected Loci Appropriate for Both  
589 Dominant and Codominant Markers: A Bayesian Perspective." *Genetics* **180**: 977-993(2008).
- 590  
591 Garrison, E. & G. Marth Haplotype-based variant detection from short-read sequencing. [preprint](https://arxiv.org/abs/1207.3907)  
592 [arXiv 1207.3907](https://arxiv.org/abs/1207.3907) (2012).
- 593  
594 Gonthier, P. & M. Garbelotto. "Amplified fragment length polymorphism and sequence analyses  
595 reveal massive gene introgression from the European fungal pathogen *Heterobasidion annosum* into  
596 its introduced congener *H. irregulare*." *Molecular Ecology* **20**: 2756-2770(2011).
- 597  
598 Gross, A., C. R. Grünig, V. Queloz, et al. "A molecular toolkit for population genetic investigations of  
599 the ash dieback pathogen *Hymenoscyphus pseudoalbidus*." *Forest Pathology* **42**: 252-264(2012).
- 600  
601 Gross, A., O. Holdenrieder, M. Pautasso, et al. "*Hymenoscyphus pseudoalbidus*, the causal agent of  
602 European ash dieback." *Molecular Plant Pathology* **15**: 5-21(2014).
- 603  
604 Gross, A., T. Hosoya & V. Queloz. "Population structure of the invasive forest pathogen  
605 *Hymenoscyphus pseudoalbidus*." *Molecular Ecology* **23**: 2943-2960(2014).

- 606  
607 Gross, A., P. L. Zaffarano, A. Duo, et al. "Reproductive mode and life cycle of the ash dieback  
608 pathogen *Hymenoscyphus pseudoalbidus*." *Fungal Genetics and Biology* **49**: 977-986(2012).
- 609  
610 Grunwald, N. J., B. A. McDonald & M. G. Milgroom. "Population Genomics of Fungal and Oomycete  
611 Pathogens." *Annual Review of Phytopathology* **54**: 323-346(2016).
- 612  
613 Guisan, A. & W. Thuiller. "Predicting species distribution: offering more than simple habitat models."  
614 *Ecology Letters* **8**: 993-1009(2005).
- 615  
616 Han, J.-G., B. Shrestha, T. Hosoya, et al. "First Report of the Ash Dieback Pathogen *Hymenoscyphus*  
617 *fraxineus* in Korea." *Mycobiology* **42**: 391-396(2014).
- 618  
619 Hietala, A. M., V. Timmermann, I. Børja, et al. "The invasive ash dieback pathogen *Hymenoscyphus*  
620 *pseudoalbidus* exerts maximal infection pressure prior to the onset of host leaf senescence." *Fungal*  
621 *Ecology* **6**: 302-308(2013).
- 622  
623 Huson, D. H. & D. Bryant. "Application of Phylogenetic Networks in Evolutionary Studies." *Molecular*  
624 *Biology and Evolution* **23**: 254-267(2006).
- 625  
626 Husson, C., O. Caël, J. P. Grandjean, et al. "Occurrence of *Hymenoscyphus pseudoalbidus* on infected  
627 ash logs." *Plant Pathology* **61**: 889-895(2012).
- 628  
629 Jakobsson, M. & N. A. Rosenberg. "CLUMPP: a cluster matching and permutation program for dealing  
630 with label switching and multimodality in analysis of population structure." *Bioinformatics* **23**: 1801-  
631 1806(2007).
- 632  
633 Kowalski, T. & O. Holdenrieder. "Pathogenicity of *Chalara fraxinea*." *Forest Pathology* **39**: 1-7(2009).
- 634  
635 Kraj, W., M. Zarek & T. Kowalski. "Genetic variability of *Chalara fraxinea*, dieback cause of European  
636 ash (*Fraxinus excelsior* L.)." *Mycological Progress* **11**: 37-45(2012).
- 637  
638 Kriticos, D. J., L. Morin, A. Leriche, et al. "Combining a Climatic Niche Model of an Invasive Fungus  
639 with Its Host Species Distributions to Identify Risks to Natural Assets: *Puccinia psidii* Sensu Lato in  
640 Australia." *PLoS ONE* **8**: e64479(2013).
- 641  
642 Leggett, R. M., R. H. Ramirez-Gonzalez, B. J. Clavijo, et al. "Sequencing quality assessment tools to  
643 enable data-driven informatics for high throughput genomics." *Frontiers in Genetics* **4**: 288(2013).
- 644  
645 Lischer, H. E. L. & L. Excoffier. "PGDSpider: an automated data conversion tool for connecting  
646 population genetics and genomics programs." *Bioinformatics* **28**: 298-299(2012).
- 647

- 648 Lockwood, J. L., P. Cassey & T. Blackburn. "The role of propagule pressure in explaining species  
649 invasions." *Trends in Ecology & Evolution* **20**: 223-228(2005).
- 650
- 651 McKinney, L. V., L. R. Nielsen, D. B. Collinge, et al. "The ash dieback crisis: genetic variation in  
652 resistance can prove a long-term solution." *Plant Pathology* **63**: 485-499(2014).
- 653
- 654 McKinney, L. V., I. M. Thomsen, E. D. Kjær, et al. "Rapid invasion by an aggressive pathogenic fungus  
655 (*Hymenoscyphus pseudoalbidus*) replaces a native decomposer (*Hymenoscyphus albidus*): a case of  
656 local cryptic extinction?" *Fungal Ecology* **5**: 663-669(2012).
- 657
- 658 McMullan, M., M. Rafiqi, G. Kaithakottil, et al. "The ash dieback invasion of Europe was founded by  
659 two individuals from a native population with huge adaptive potential." *Nature Ecology and  
660 Evolution*(submitted).
- 661
- 662 Narum, S. R. & J. E. Hess. "Comparison of FST outlier tests for SNP loci under selection." *Molecular  
663 Ecology Resources* **11**: 184-194(2011).
- 664
- 665 Paini, D. R., A. W. Sheppard, D. C. Cook, et al. "Global threat to agriculture from invasive species."  
666 *Proceedings of the National Academy of Sciences* **113**: 7575-7579(2016).
- 667
- 668 Pfeifer, B., U. Wittelsbürger, S. E. Ramos-Onsins, et al. "PopGenome: An Efficient Swiss Army Knife for  
669 Population Genomic Analyses in R." *Molecular Biology and Evolution* **31**: 1929-1936(2014).
- 670
- 671 Pritchard, J. K., M. Stephens & P. Donnelly. "Inference of population structure using multilocus  
672 genotype data." *Genetics* **155**: 945-959(2000).
- 673
- 674 Przybył, K. "Fungi associated with necrotic apical parts of *Fraxinus excelsior* shoots." *Forest Pathology*  
675 **32**: 387-394(2002).
- 676
- 677 Robin, C., A. Andanson, G. Saint-Jean, et al. "What was old is new again: thermal adaptation within  
678 clonal lineages during range expansion in a fungal pathogen." *Molecular Ecology* **26**: 1952-  
679 1963(2017).
- 680
- 681 Roper, M., A. Seminara, M. M. Bandi, et al. "Dispersal of fungal spores on a cooperatively generated  
682 wind." *Proceedings of the National Academy of Sciences* **107**: 17474-17479(2010).
- 683
- 684 Rytkönen, A., A. Lilja, R. Drenkhan, et al. "First record of *Chalara fraxinea* in Finland and genetic  
685 variation among isolates sampled from Åland, mainland Finland, Estonia and Latvia." *Forest  
686 Pathology* **41**: 169-174(2011).
- 687
- 688 Saunders, D., K. Yoshida, C. Sambles, et al. "Crowdsourced analysis of ash and ash dieback through  
689 the Open Ash Dieback project: A year 1 report on datasets and analyses contributed by a self-  
690 organising community." *bioRxiv*, 004564 (2014).

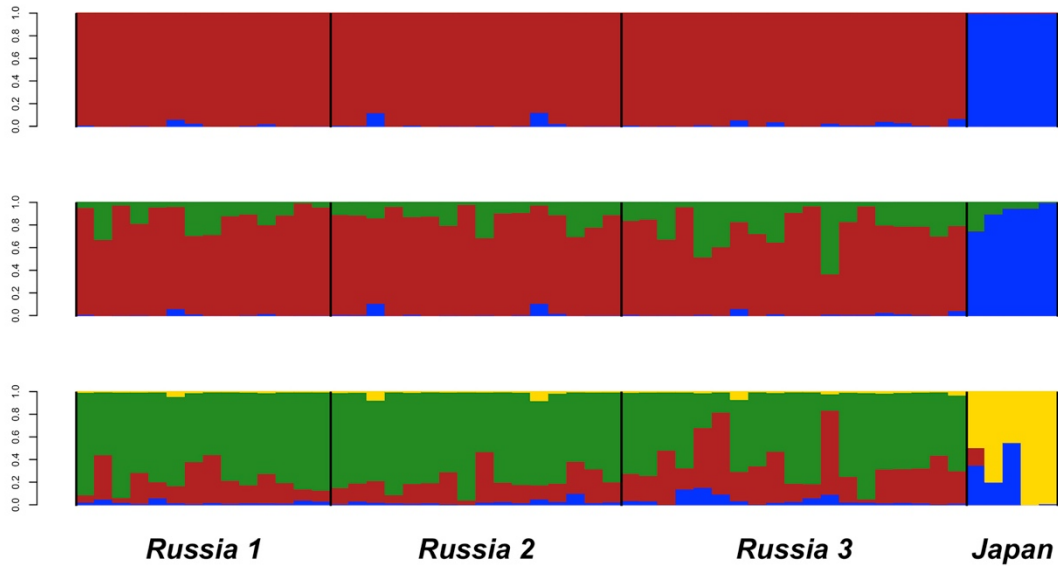
- 691  
692 Schoebel, C. N., L. Botella, V. Lygis, et al. "Population genetic analysis of a parasitic mycovirus to infer  
693 the invasion history of its fungal host." *Molecular Ecology* **26**: 2482-2497(2017).
- 694  
695 Skovsgaard, J. P., I. M. Thomsen, I. M. Skovgaard, et al. "Associations among symptoms of dieback in  
696 even-aged stands of ash (*Fraxinus excelsior* L.)." *Forest Pathology* **40**: 7-18(2010).
- 697  
698 Solheim, H. & A. M. Hietala. "Spread of ash dieback in Norway." *Baltic Forestry* **23**: 144-149(2017).
- 699  
700 Stukenbrock, E. H., T. Bataillon, J. Y. Dutheil, et al. "The making of a new pathogen: Insights from  
701 comparative population genomics of the domesticated wheat pathogen *Mycosphaerella graminicola*  
702 and its wild sister species." *Genome Research* **21**: 2157-2166(2011).
- 703  
704 Stukenbrock, E. H., F. B. Christiansen, T. T. Hansen, et al. "Fusion of two divergent fungal individuals  
705 led to the recent emergence of a unique widespread pathogen species." *Proceedings of the National*  
706 *Academy of Sciences* **109**: 10954-10959(2012).
- 707  
708 Timmermann, V., I. Børja, A. M. Hietala, et al. "Ash dieback: pathogen spread and diurnal patterns of  
709 ascospore dispersal, with special emphasis on Norway." *EPPO Bulletin* **41**: 14-20(2011).
- 710  
711 Tollefsrud, M. M., T. Myking, J. H. Sønstebo, et al. "Genetic Structure in the Northern Range Margins  
712 of Common Ash, *Fraxinus excelsior* L." *PLOS ONE* **11**: e0167104(2016).
- 713  
714 Van Kan, J. A. L., J. H. M. Stassen, A. Mosbach, et al. "A gapless genome sequence of the fungus  
715 *Botrytis cinerea*." *Molecular Plant Pathology* **18**: 75-89(2017).
- 716  
717 Wey, T., M. Schlegel, S. Stroheker, et al. "MAT--gene structure and mating behavior of  
718 *Hymenoscyphus fraxineus* and *Hymenoscyphus albidus*." *Fungal Genetics and Biology* **87**: 54-  
719 63(2016).
- 720  
721 Zhan, A., J. A. Darling, D. G. Bock, et al. "Complex genetic patterns in closely related colonizing  
722 invasive species." *Ecology and Evolution* **2**: 1331-1346(2012).
- 723  
724 Zhao, Y.-J., T. Hosoya, H.-O. Baral, et al. "*Hymenoscyphus pseudoalbidus*, the correct name for  
725 *Lambertella albida* reported from Japan." *Mycotaxon* **122**: 25-41(2013).
- 726  
727 Zheng, H.-D. & W.-Y. Zhuang. "*Hymenoscyphus albidoides* sp. nov. and *H. pseudoalbidus* from China."  
728 *Mycological Progress* **13**: 625-638(2014).
- 729  
730 Zheng, X., D. Levine, J. Shen, et al. "A high-performance computing toolset for relatedness and  
731 principal component analysis of SNP data." *Bioinformatics* **28**: 3326-3328(2012).
- 732

733 **Figures**



734

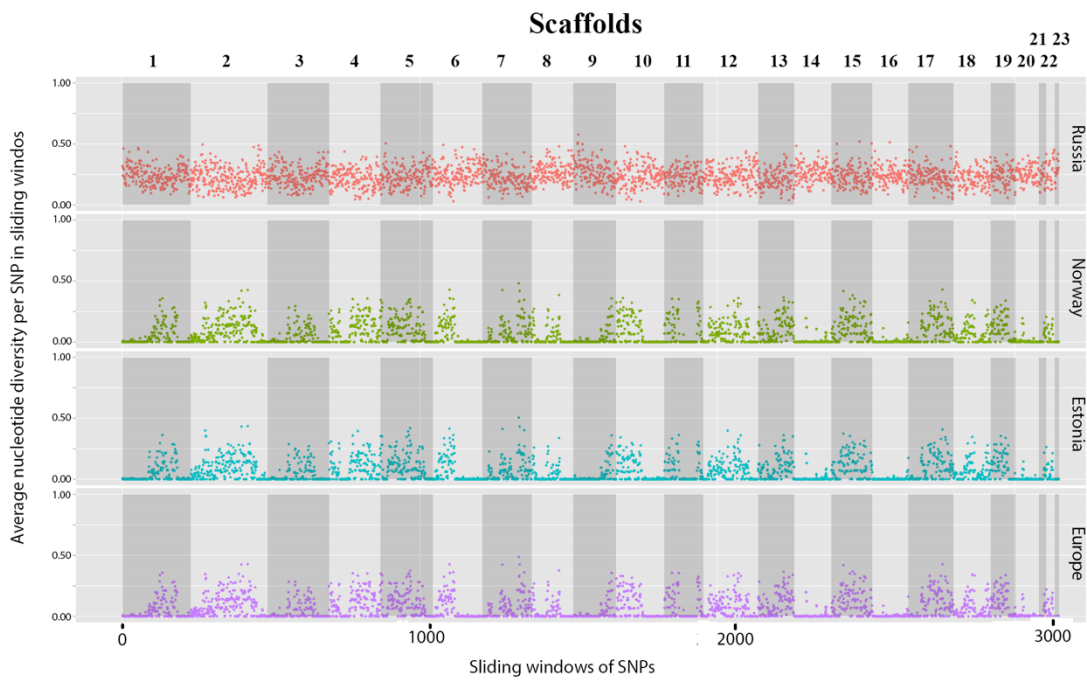
735 **Figure 1: Sampling locations and relationship among isolates of *Hymenoscyphus fraxineus* and *H. albidus*.** Map of  
736 sampling locations in Europe (A) and Asia (B). Principle component analysis of *H. fraxineus* and *H. albidus* (C) and *H.*  
737 *fraxineus* only (D). The percentage of variance held by each eigenvector is written on the axis. The first eigenvector splits *H.*  
738 *albidus* and *H. fraxineus*, while the second splits the Asian and the European populations of *H. fraxineus*. The SplitsTree,  
739 neighbor-net analysis of *H. fraxineus* (E) shows the same pattern of relationship between the different populations as the  
740 PCA where the European samples (blue) are separated from the Russian (red) and the Japanese (green).



741

742 Figure 2: **Population structure of Asian *Hymenoscyphus fraxineus*.** Structure analysis of the Asian *H. fraxineus* individuals  
743 shows the membership in different genetic groups at K=2 (top), K=3 (middle) and K=4 (bottom).

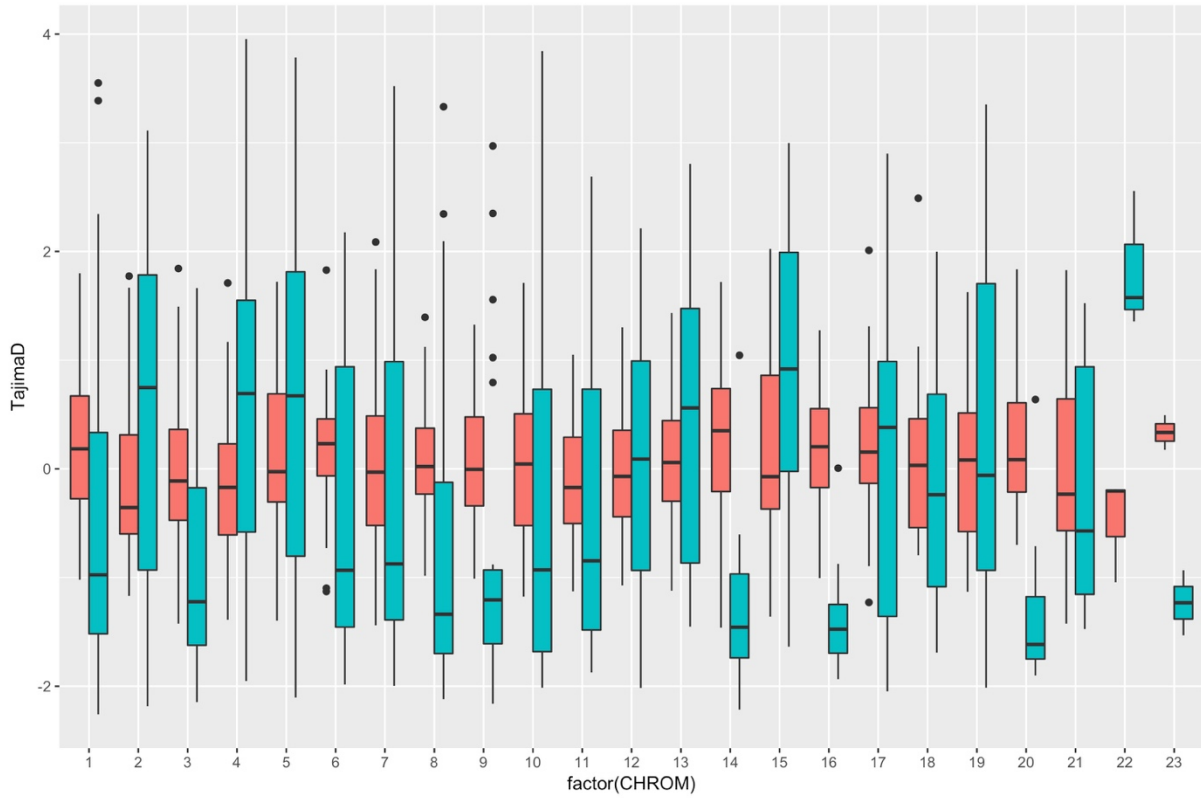
744



745

746 Figure 3. **Genome-wide diversity of *Hymenoscyphus fraxineus*.** Nucleotide diversity per SNP calculated in sliding windows  
747 of seven SNPs with five SNPs jumps in the Russian Far East, Norwegian, Estonian and remaining European individuals.

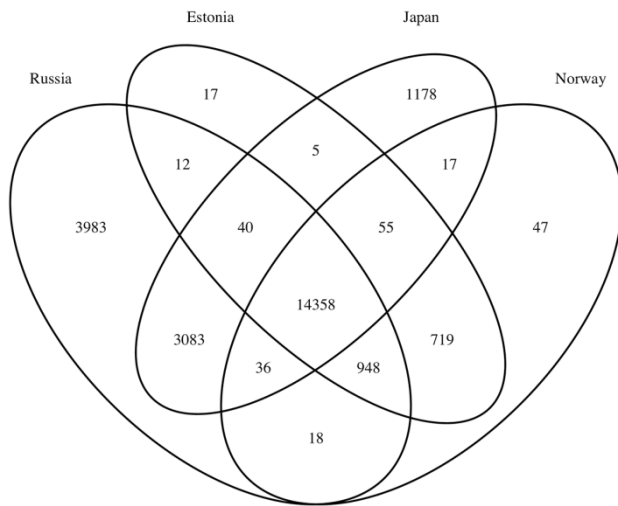
748



749

750  
751

Figure 4. **Tajima's D for each scaffold.** The Tajima's D was calculated for the combined *H. fraxineus* from Asia (red) and Europe (green).



752

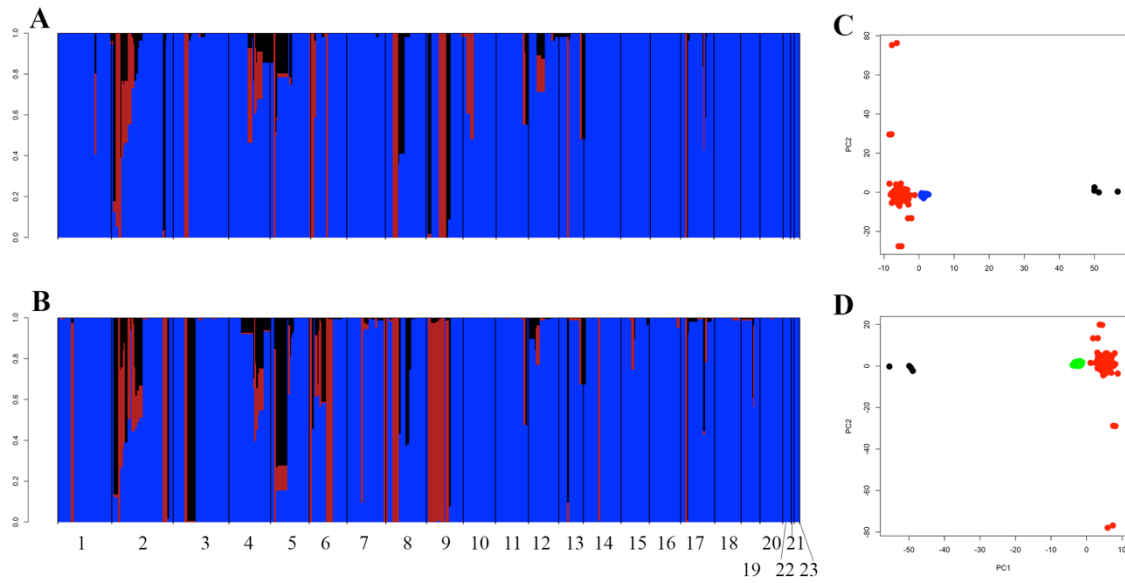
753  
754

Figure 5. **Distribution of alleles among sampling locations of *H. fraxineus*.** The Venn diagram shows the distribution of alleles with frequency above 0.05 in *H. fraxineus* from Russia, Estonia, Japan and Norway.

755

756





757

758 Figure 6: **Local ancestry assignment of Estonian and Norwegian *H. fraxinues* individuals.** The PCAdmix analyses give the  
759 average ancestry in windows of 10 SNPs along the genome (Russian ancestry in blue, Japanese ancestry in red and with  
760 uncertain ancestry in black) in (A) Estonian individuals and (B) Norwegian individuals. (C) and (D) show the average loadings  
761 for the first two principle components axes for (A) and (B) respectively (Russian haplotypes are in red, Japanese haplotypes  
762 are in black, Estonian haplotypes are in blue and Norwegian haplotypes are in green).

763